Physica B 185 (1993) 234–238
North-Holland

PHYSICA B

Site-selective study of picosecond relaxation processes of Ni^{2+} in polymorphic ZnS

R. Heitz, L. Eckey, A. Hoffmann and I. Broser
Institut für Festkörperphysik, Technische Universität, Berlin, Germany

The time dependence of the $^3T_1(P)$–$^3T_1(F)$ luminescence of Ni^{2+} centres in polymorphic ZnS crystals is investigated. By means of time- and site-selective spectroscopy both decay and thermalization processes in the ps-domain are demonstrated. Especially, the interaction with low-frequency phonons is altered by changes in the local environment of the Ni^{2+} ion.

1. Introduction

Transition metals are well known as efficient 'killer' centres in semiconductors. Due to their amphoteric behaviour they exhibit strong electrical activity and offer an enormous potential for technical application in semiconductor devices. Nevertheless, there is still a lack of detailed information on the recombination processes involved. Recently, radiative relaxation processes on a ps time scale have been observed at Ni^{2+} centres in wide-band-gap II–VI semiconductors [1]. These fast luminescence kinetics have been successfully used to study the electronic coupling between the Ni^{2+} centre and the host bands [2]. Hole capture times down to 30 ps have been found. The purpose of this paper is to study the dynamics of Ni^{2+} emissions in ZnS in more detail. The polymorphic crystal structure of ZnS offers the possibility to investigate the influence of only slightly different environments on decay and thermalization processes of Ni^{2+} states. The results are discussed in view of the varying C_{3V} crystal field of the different axial centres.

2. Experimental setup

The crystals are grown from the gaseous phase by the Frerich–Warminsky method [3] and subsequently doped by indiffusion with up to 1 ppm Ni. A tuneable dye laser (DCM) synchronously pumped by an actively modelocked Nd:YAG laser provided ps-pulses (4 ps) in the spectral region of the Ni^{2+} ($^3T_1(F)$–$^1T_2(G)$) absorption. The crystals were immersed in superfluid He at 1.8 K. The Ni^{2+} ($^3T_1(P)$–$^3T_1(F)$) luminescence was detected through a subtractive 0.35 m double monochromator using time-correlated single-photon counting techniques. As detector served a double-stage multi-channel-plate photomultiplier with an extended-red photocathode. A time resolution better than 10 ps is obtained by means of deconvolution techniques. Exponential rise (τ_r) and decay (τ_d) processes are assumed for the transients which is reasonable with regard to the atomic-like character of the transitions involved.

Correspondence to: R. Heitz, Sekr. PN5-3, Institut für Festkörperphysik, Technische Universität Berlin, Hardenbergstrasse 36, 1000 Berlin 12, Germany.

3. The fine structure

Ni^{2+} has an electronic d^8 configuration leading to a wealth of states in a T_d crystal field. A rough term scheme containing the states and the optical transitions of interest in the present context is given in fig. 1. The $^3T_1(P)$ term has the fine structure levels T_2, E, A_1 resulting from spin–orbit interaction altered by a dynamical Jahn–Teller coupling to T_2 modes [4,5]. Including a C_{3V} crystal field the T_2 state is split into two components (A_1, E). In the $^3T_1(F)$ term a T_1

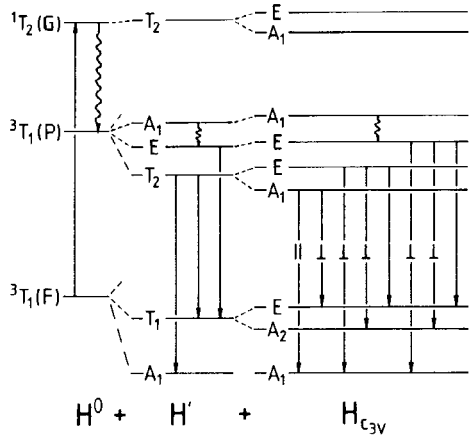

Fig. 1. Schematic term scheme of Ni^{2+} (d^8 configuration) in T_d and C_{3V} symmetry. H^0 contains the electron–electron interaction and the T_d crystal field, H' contains the spin–orbit interaction and a dynamical Jahn–Teller coupling to T_2 modes, $H_{C_{3V}}$ represents the trigonal crystal field of the axial centres. The excitation and relaxation processes involved in the time- and site-selective measurements are indicated.

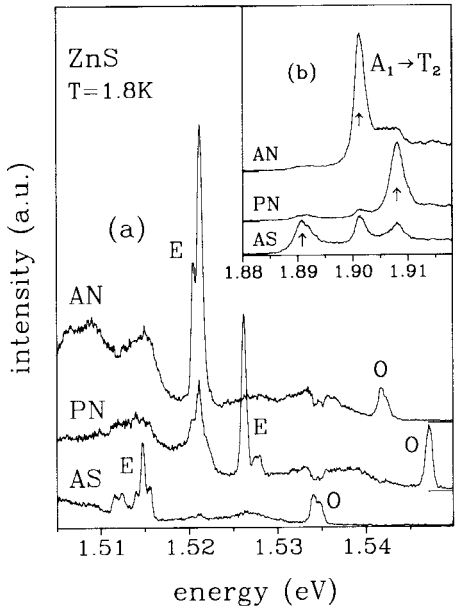

Fig. 2. Site-selective luminescence (a) and excitation (b) spectra of different Ni^{2+} centres in polymorphic ZnS. The $^3T_1(P)$–$^3T_1(F)$ luminescences are excited via the A_1–T_2 ZPLs and the dominating E ZPLs have been detected for the excitation spectra in the region of the $^3T_1(F)$–$^1T_2(G)$ transition.

state or, respectively, its two C_{3V} components A_2 and E lie above the A_1 ground state. In general, optical spectra of Ni^{2+} in ZnS are much more complicated than expected from the term scheme, fig. 1. The polymorphic crystal structure provides different environments for point defects, forming so-called axial sites with their c-axis corresponding to the cubic $[1\,1\,1]_{growth}$-axis. A simple classification scheme considers only four stacking layers around the impurity leading to the four main centres, the cubic AN, the axial PN as well as AS and the hexagonal PS centres [6]. Including more distant stacking layers additional subcentres can be distinguished. For the $^3T_1(F)$–$^3T_1(P)$ transition in ZnS zero phonon lines (ZPLs) of at least two additional axial sites are observed beside those of the cubic one [7]. A detailed investigation of these axial centres is under way [8] showing the PN centre to be shifted by 5.84 meV to higher and the AS centre by −8.09 meV to lower energies with respect to the cubic AN centre.

In the present work the $^3T_1(F)$–$^1T_2(G)$ absorption is used to excite the $^3T_1(P)$–$^3T_1(F)$ luminescence under investigation. Figure 2 shows luminescence (a) and excitation (b) spectra in the regions of the $^3T_1(P)$–$^3T_1(F)$ and $^3T_1(F)$–$^1T_2(G)$ transitions, respectively, of the AN, PN and AS centres. As is obvious from fig. 2 the experimental setup chosen allows selective excitation of the different axial centres in polymorphic ZnS, which is very useful for the time-resolved measurements below. The excitation spectra (fig. 2(b)) reveal the polytypes in the $^3T_1(F)$–$^1T_2(G)$ transition for the first time. The PN ZPL is shifted by 6.9 meV to higher and the AS ZPL by −10.5 meV to lower energies with respect to the cubic AN ZPL. The A_1–T_2 ZPLs are of almost Lorentzian shape with half widths (FWHM) of 2.2 meV for the AN and 3.0 meV for the axial PN and AS centres. The larger half widths of the axial ZPLs may be caused by the C_{3V} crystal field splitting of the excited T_2 state.

Exciting resonantly the different Ni^{2+} centres (fig. 2(a)) their luminescences are almost completely separated, all showing a similar fine structure. They start with ZPLs corresponding to the respective O-absorptions. Additionally, the O-absorptions of the AS centre appear in the

luminescences of the AN and PN centres. Towards lower energies a more complicated structure is observed, consisting of a doublet for the AN-centre and even more lines for the axial ones. These line structures will be named E lines in the following and are due to transitions from the energetically lowest E and $T_2(A_1, E)$ states of the excited $^3T_1(P)$ term into the $T_1(A_2, E)$ state as indicated in fig. 1. Those emissions originating at the excited E state are 'hot' lines. In thermal equilibrium at $T = 1.8$ K the E states, lying nearly 1 meV above the T_2 states, should not be populated. This assignment is confirmed by magneto-optical results [8]. In general, it is difficult to observe the E lines of the AS centre, since they are superimposed on the strong acoustical phonon sideband of the cubic AN centre and accidently almost coincide with the ZPLs of the $W^{2+}(^3T_1-^1A_1)$ transition [9] around 1.5115 eV. Nevertheless, this line group consists of at least 3 doublets originating at different subcentres. The fine structure of the main axial centres AN, PN, and AS in polymorphic ZnS is listed in table 1 (T_2^* gives the mean energy of the $T_2(A_1, E)$ doublet).

The structure of the Ni^{2+} centre is altered by nearby stacking faults. Despite the C_{3V} splitting of the T_2 state the level separations in the $^3T_1(P)$ term increase generally, which indicates a stabilization of the centre against Jahn–Teller distortions in axial environments. But the main effect is a shift of the whole fine structure. This shift results from changes in the T_d crystal field strength caused by the variation of the cluster size [10]. Thus, comparing with results of recent hydrostatic-pressure measurements [11] the shifts of the $^3T_1(F)-^1T_2(G)$ transition can be extrapolated to be about twice as large as those of the $^3T_1(F)-^3T_1(P)$ transition. In fact, they are just 1.2 to 1.3 times larger. The difference should result from the stabilization of the $^3T_1(P)$ state by the C_{3V} crystal field, too, leading to larger shifts in the $^3T_1(F)-^3T_1(P)$ transition.

4. The time dependence

Figure 3 gives time-delayed luminescence spectra showing the E-line doublet of the cubic AN centre. Both lines decay within 600 ps, clearly demonstrating the ps character of the $Ni^{2+}(^3T_1(P)-^3T_1(F))$ transition in ZnS. Even though both belong to the same center the 'hot' $E-T_1$ line decays slightly faster than the T_2-T_1 line. There is no complete thermalization in the excited $^3T_1(P)$ state during its lifetime. Despite

Table 1
Fine structure of the cubic AN and the axial PN as well as AS centres in polymorphic ZnS (T_2^* gives the mean of the $T_2(A_1, E)$ doublet). The decay times τ_d of the fine structure states of the $^3T_1(P)$ and the $^1T_2(G)$ terms are given.

	$^3T_1(F)$		$^3T_1(P)$			$^1T_2(G)$		
		E (meV)		E (meV)	τ_d (ps)		E (meV)	τ_d (ps)
AN	A_1	0	T_2	1541.29	100	T_2	1910.8	10
	T_1	+22.11	E	+0.83	70			
			A_1	+1.83	–			
PN	A_1	0	T_2^*	1547.13	125	T_2^*	1917.7	10
	A_2	+20.96	A_1	−0.14				
	E	+21.79	E	+0.07				
			E	+1.09	45			
			A_1	+2.21	–			
AS	A_1	0	T_2^*	1533.20	115	T_2^*	1900.3	10
	A_2	+20.1	E	−0.11				
	E	+22.4	A_1	+0.21				
			E	+0.96	–			
			A_1	+2.09	–			

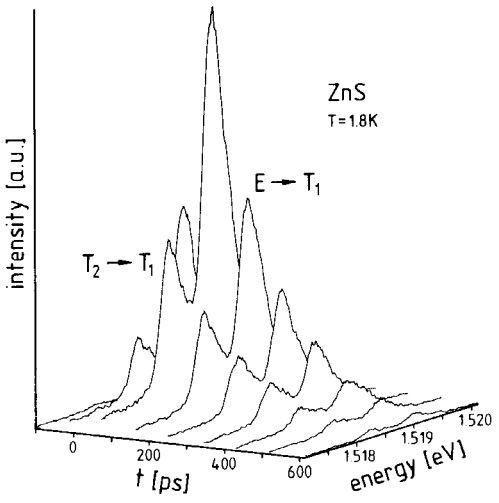

Fig. 3. Time-delayed spectra of the E doublet of the Ni^{2+} ($^3T_1(P)$–$^3T1(F)$) luminescence of the cubic AN centre in ZnS. Subsequent time windows of 80 ps duration are used.

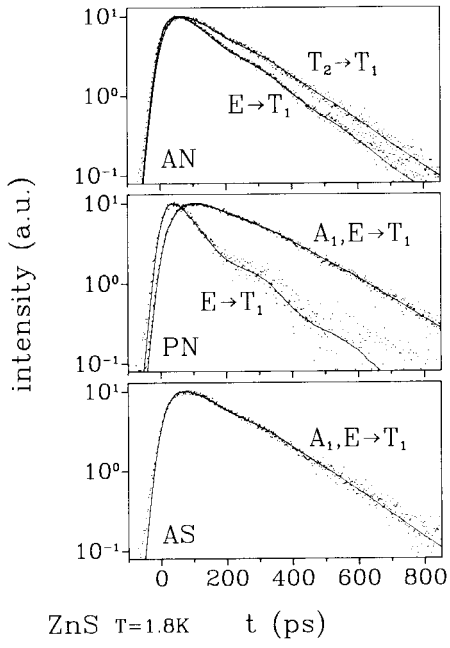

Fig. 4. Luminescence transients of the E-lines of different Ni^{2+} centres in polymorphic ZnS. Transients of ZPLs originating from different excited fine-structure states are shown.

the optical relaxation, thermalization processes between the lowest components of the $^3T_1(P)$ term also have to be taken into account to explain the time behaviour of the different ZPLs.

Figure 4 shows transients of the cubic AN and both the axial PN and AS centres recorded under selective excitation via the respective A_1–T_2 ZPL of the $^3T_1(F)$–$^1T_2(G)$ absorption. Some representative ZPLs are chosen. The solid lines represent fits obtained after convolution of the apparatus response with two-exponential transients. All lines except those originating at the $T_2(A_1, E)$ doublet of the PN centre show rise processes with a 10 ps time constant. This is the relaxation time from the optically excited $^1T_2(G)$ to the luminescent $^3T_1(P)$ state under investigation [2], which is the same for all axial centres. In contrast, the $T_2(A_1, E)$–T_1 transition of the PN centre rises with a time constant of 40 ps, which is the decay time of the E–T_1 transition, too. This means that the $T_2(A_1, E)$ doublet is populated via the E state by the emission of low-frequency phonons. For the AS centre no ZPL originating at the E state is observed indicating an even faster relaxation process. A lower limit of 8 ps for the time constant is given by the FWHM of the A_1–E absorption of 80 μeV.

The decay times τ_d of the different ZPLs are given in table 1 for the respective excited state. The decay times are in the order of 100 ps, with the $T_2(A_1, E)$-states of the axial PN and AS centres decaying more slowly than that of the cubic AN centre. For the cubic AN and the axial AS centres ZPLs of the subcentres could be resolved which behave similarly to the main centres. Additionally, both C_{3V} components of the T_2 states of the axial centres show the same time behaviour.

d–d transitions of transition metals are dipole-forbidden by parity from an atomic point of view, but become allowed by the interaction with the host crystal. The covalent bonding as well as the intracentre term interaction caused by the T_d crystal field remove this selection rule. However, in general lifetimes between some ms and some hundred ns are reported for such such transitions [12]. Ni^{2+} in the wide-band-gap II–VI semiconductors [1] offers exceptionally high radiative

transition probabilities. However, competing nonradiative processes contribute to the decay times in the ps-range as has been shown by calorimetric absorption spectroscopy [13]. Quantum efficiencies around 10% have been determined for the $^3T_1(P)$–$^3T_1(F)$ transition [1].

Time-resolved studies of the $^4T_1(G)$–$^6A_1(S)$ luminescences of Mn^{2+} and Fe^{3+} in ZnS revealed shorter time constants for the axial centres than for the cubic one [14,15]. This is in contrast to the case of Ni^{2+} discussed here. Whereas for the spin- and symmetry-forbidden $^4T_1(G)$–$^6A_1(S)$ transition the additional C_{3V} crystal field removes selection rules, this is not the case for the overall allowed $^3T_1(P)$–$^3T_1(F)$ transition. The second noticeable trend is more surprising. Obviously, the electron–phonon interaction changes drastically, leading to much faster thermalization processes in the axial centres. One reason may be the separation between the lowest component and the E-state increasing from 830 μeV (AN) over 1220 μeV (PN) to 1280 μeV (AS). The one-phonon density increases with $(\hbar\omega)^2$ connected with increasing relaxation probabilities caused by resonant one-phonon processes [16]. Also, it is possible that low-energy local modes are involved which slightly mismatch the energy distance in the cubic centre or change their energy with the local environment of the Ni ion.

5. Conclusions

Luminescence dynamics with time constants around 100 ps of inner d–d transitions of Ni^{2+} centres in ZnS are demonstrated. The C_{3V} crystal field of the axial centres increases the lifetime of the $^3T_1(P)$ state. The observation of 'hot' ZPLs shows that the emission of low-frequency optical phonons takes place on a similar time scale depending strongly on the local environment of the Ni^{2+} ion.

References

[1] R. Heitz, A. Hoffmann and I. Broser, Opt. Mater. 1 (1992) 75.
[2] R. Heitz, A. Hoffmann and I. Broser, J. Lumin. 53 (1992) 359.
[3] I. Broser and R. Broser, Deutsches Patentamt, Patentschrift Nr. 814193 (1950).
[4] U. Kaufmann and P. Koidl, J. Phys. C 7 (1974) 791.
[5] B. Nestler, A. Hoffmann, L.B. Xu, U. Scherz and I. Broser, J. Phys. C 20 (1987) 4613.
[6] B. Lambert, T. Buch and A. Geoffroy, Phys. Rev. B 8 (1973) 863.
[7] I. Broser, A. Hoffmann, R. Germer, R. Broser and E. Birkicht, Phys. Rev. B 33 (1986) 8196.
[8] R. Heitz, A. Hoffmann and I. Broser, to be published.
[9] R. Heitz, P. Thurian, A. Hoffmann and I. Broser, Mater. Sci. Forum 83–87 (1992) 1247.
[10] R. Parrot, A. Geoffroy, C. Naud, W. Busse and H.-E. Gumlich, Phys. Rev. B 23 (1981) 5288.
[11] D. Wasik, Z. Liro and M. Baj, Proceedings of the 19th ICDS 1988, Warschau, ed. W. Zawadzki, Institute of Physics, Polish Academy of Science (1988) p. 1197.
[12] G. Goetz and H.-J. Schulz, J. Lumin. 40–41 (1988) 415.
[13] L. Podlowski, R. Heitz, A. Hoffmann and I. Broser, J. Lumin. 53 (1992) 401.
[14] W. Busse, H.-E. Gumlich, W. Knaak and J. Schulz, J. Phys. Soc. Japan A 49 (1980) 581.
[15] A. Hoffmann, R. Heitz and I. Broser, Phys. Rev. B 41 (1990) 5806.
[16] B. di Bartolo, Optical Interactions in Solids (Wiley, New York, 1968) p. 343.